

# Molecular Analysis of the Feline Immunodeficiency Virus Protease: Generation of a Novel Form of the Protease by Autoproteolysis and Construction of Cleavage-Resistant Proteases

GARY S. LACO,<sup>1</sup> MICHAEL C. FITZGERALD,<sup>2</sup> GARRET M. MORRIS,<sup>1</sup> ARTHUR J. OLSON,<sup>1</sup>  
STEPHEN B. H. KENT,<sup>3</sup> AND JOHN H. ELDER<sup>1\*</sup>

*Department of Molecular Biology<sup>1</sup> and Department of Cell Biology,<sup>2</sup> The Scripps Research Institute, La Jolla, California 92037, and Gryphon Sciences, South San Francisco, California 94080<sup>3</sup>*

Received 6 January 1997/Accepted 4 April 1997

**The feline immunodeficiency virus (FIV) protease is essential for virion maturation and subsequent viral replication in that it cleaves the Gag and Gag/Pol polyproteins at eight sites to release the respective structural proteins and enzymes. During purification of a recombinant FIV protease (PR), we noted that it underwent autoproteolysis (autolysis) to give discrete cleavage products. These additional PR cleavage sites were defined using N-terminal amino acid sequence analysis and mass spectrometry. Protease breakdown products were also found in FIV virions and were of the same apparent molecular weights as the in vitro autolysis products. Four primary PR autolysis sites were blocked via substitution of either the P1 amino acid with a  $\beta$ -branched amino acid or the P1' amino acid with lysine. Cleavage-resistant PRs which had  $K_m$  and  $k_{cat}$  values similar to those of FIV PR were constructed. An autolysis time course determined that blocking all four primary autolysis sites yielded a cleavage-resistant PR which was enzymatically stable. Concomitant with autolysis is the generation of an N-terminally truncated form of the PR (Thr6/PR) which has enhanced stability with respect to that of FIV PR. A structural basis for the Thr6/PR activity is presented, as are the possible roles of autolysis in the viral replication cycle.**

Feline immunodeficiency virus (FIV) is the causative agent of an immune deficiency syndrome in cats, the disease symptoms and progression of which parallel those of human immunodeficiency virus (HIV) in humans (20). The FIV genome organization and encoded proteins are also similar to those of HIV and other lentiviruses, including a symmetrical dimeric aspartic protease (PR) (34). Although differences exist relative to the presence or absence of several small open reading frames (ORFs), both FIV and HIV express the viral structural proteins and enzymes as part of the Gag and Gag/Pol polyproteins (6, 13). The N-myristoylated Gag and Gag/Pol polyproteins and the Env glycoprotein make their way to the plasma membrane of the infected cell, where the immature virion assembles and then buds off (3, 6, 10). The monomeric PR in the Gag/Pol polyproteins dimerizes during the budding process, perhaps due to an increase in the local concentration of the enzyme (23) and/or a change in the local ionic strength (4). The active PR dimer, as part of the Gag/Pol polyprotein, then processes PR subunits out of the polyproteins, resulting in maturation of the virion and activation of several key enzymes, including reverse transcriptase (13). This allows FIV, and similarly HIV, to initiate a productive replication cycle in a newly infected cell. PR is a key component of the FIV and HIV replication cycles in that it not only regulates virion maturation and activity of viral enzymes but also, with HIV and simian immunodeficiency virus (SIV), regulates its own activity in vitro through autoproteolysis (autolysis) (17, 25). However, it is not known if autolysis of either HIV or SIV PRs occurs in vivo and whether it has a role in the virus replication cycle.

In the case of pepsin, a mammalian gastric protease, autolysis is important for removal of an N-terminal inhibitory domain from the zymogen (pepsinogen), resulting in active pepsin. Subsequently, pepsin undergoes further autolysis which inactivates the protease (8, 22). Thus, autolysis controls an inherently nonspecific protease which, if unchecked, could damage intestinal tissues after secretion and activation (16, 31).

We have studied the FIV PR to determine if it undergoes autolysis in vitro and in vivo. In this report, we describe in vitro four primary autolysis sites within FIV PR and show that FIV virions also contain PR breakdown products. These autolysis sites were blocked in vitro by specific amino acid substitutions at either the P1 or P1' position of the cleavage sites. Blocking all four autolysis sites resulted in a PR highly resistant to autolysis and enzymatically stable. In addition, we generated by autolysis a novel truncated form of FIV PR (Thr6/PR) which is resistant to subsequent autolysis and retains greater activity at high urea concentrations than does FIV PR. The role of the FIV PR three-dimensional structure in regulating autolysis is discussed.

## MATERIALS AND METHODS

**Protease constructs.** (i) **pT7-FIV PR.** The FIV 34TF10 infectious molecular clone (FIV-34TF10 [30]) was used as the template in a PCR using a positive-strand primer (5'ACTATGGACATATGGCATATAATAAAGTAGGTACTACTAC3'; nucleotides [nt] 1964 to 2005) which, when incorporated into the PCR product, added an initiation Met and Ala codon to the determined 5' Tyr codon of the FIV PR ORF (6) as well as a 5' *NdeI* restriction site. A negative-strand primer (5'ATCAGAAAGCTTTTACATTACTAACCTGATATTAATTT3'; complementary to nt 2306 to 2345) added a stop codon after the determined C-terminal Met codon of the PR ORF (6) in addition to a 3' *HindIII* restriction site, to facilitate cloning. The resulting PCR product was digested with *NdeI* and *HindIII* and ligated into pT7-7 (29), which had been digested with *NdeI* and *HindIII*, to give pT7-FIV PR.

\* Corresponding author. Mailing address: The Scripps Research Institute, MB-14, 10550 North Torrey Pines Rd., La Jolla, CA 92037. Phone: (619) 784-8270. Fax: (619) 784-2750.

(ii) **pT7-Thr6/PR.** FIV-34TF10 was the template in a PCR with a positive-strand primer (5'TATAATAAACATATGACTACTACAACATTAGAAAAAGG3'; nt 1982 to 2020) which added an *NdeI* restriction site and an initiation Met codon 5' to the PR ORF Thr 6 codon. The negative-strand primer was the same as used for generation of pT7-FIV PR. The PCR product was digested with *NdeI* and *HindIII* and ligated into pET-21 (Novagen) which had been digested with *NdeI* and *HindIII*.

(iii) **pT7-G5I/PR.** FIV-34TF10 was the template in a PCR using a positive-strand primer (5'ACTATTGGACATATGGCATATAATAAGTAATAACTACTACAACATTAGAAAAAGG3'; nt 1964 to 2020) which added an *NdeI* restriction site, initiation Met, and Ala codon 5' to the determined N-terminal Tyr codon of the FIV PR ORF and changed the PR Gly 5 codon (see Fig. 2) to an Ile codon. The negative-strand primer was the same as that used for pT7-FIV PR. The resulting PCR product was digested with *NdeI* and *HindIII* and ligated into pT7-7 as described above.

(iv) **pT7-N55T/PR.** FIV-34TF10 was the template in a PCR with a positive-strand primer (5'TCTATAGAAAATGGAAGGCCAAACAATGATTGGAGTAGGAGGAGAAAGAGAGGAAC3'; nt 2124 to 2179), which mutated the PR ORF Asp 55 codon to a Thr codon, and the negative-strand primer used for pT7-FIV PR. The resulting PCR product was purified and used in a second PCR as the negative-strand primer; the positive-strand primer was that used for the pT7-FIV PR construct. The resulting PCR product was digested with *NdeI* and *HindIII* and ligated into pT7-7 as described above.

(v) **pT7-C84K/PR.** FIV-34TF10 was the template in a PCR with a negative-strand primer (5'CATAGACACAAACATTACCAATATTTTTGTGTCTTATAATTTTCATCTCT3'; complementary to nt 2207 to 2258) which mutated the PR ORF Cys 84 codon to a Lys codon; the positive-strand primer was that used to construct pT7-FIV PR. The resulting PCR product was purified and used in a second PCR as the positive-strand primer, with the same negative-strand primer as used for the pT7-FIV PR construct. The resulting PCR product was digested with *NdeI* and *HindIII* and ligated to pT7-7 as described above.

(vi) **pT7-2X/PR.** pT7-N55T/PR was digested with *EcoRV* and *HindIII*. The ~250-bp restriction fragment containing the 3' two-thirds of the N55T/PR ORF was purified and ligated to pT7-G5I/PR, which had been digested with *EcoRV* and *HindIII* to remove the 3' two-thirds of the G5I/PR ORF. This resulted in pT7-2X/PR, which contains the G5I and N55T mutations.

(vii) **pT7-3X/PR.** pT7-2X/PR was digested with *BsrGI* and *HindIII*, and the ~2,700-bp fragment (vector and 5' two-thirds of the insert) was ligated to a ~200-bp restriction fragment derived from pT7-C84K/PR which had been digested with *BsrGI* and *HindIII*. The resulting construct, pT7-3X/PR, contains the G5I, N55T, and C84K codon mutations.

(viii) **pT7-D30N/PR.** FIV-34TF10 was used as the template in a PCR with primer 5'PR/D30N (5'CCTATAAAATTTTTATTAAACACAGGAGCAGATATAACAATT3'; FIV-34TF10 nt 2051 to 2093), which mutates the FIV PR aspartic acid codon 30 to an asparagine, and the same negative-strand primer as used for the pT7-FIV PR construct. The resulting ~300-bp PCR product was used in a second PCR with the same positive-strand primer as used for the pT7-FIV PR construct. The resulting PCR product was digested with *NdeI* and *HindIII* and ligated into pT7-7 which had been digested with *NdeI* and *HindIII*, resulting in pT7-D30N/PR.

All clones were sequenced to confirm the modifications made to the FIV PR ORF.

**Protease expression.** All PR expression constructs were transformed into *Escherichia coli* BL21(DE3) (28), which contains the T7 polymerase gene under control of the *lac* promoter, as well as the pLysS plasmid, which contains the lysozyme gene under control of a constitutive promoter. Cultures were induced at an optical density at 600 nm of 0.5 with 1 mM isopropylthiogalactopyranoside for 5 h; cells were pelleted and resuspended in 10 mM Tris (pH 8.0)–5 mM EDTA and frozen at  $-70^{\circ}\text{C}$ . The cell solution was then thawed, resulting in cell lysis. The cellular DNA was sheared in a Waring blender for 10 s; Nonidet P-40 was added to 0.1% followed by urea to 2 M. The solution was then centrifuged at  $5,000 \times g$  to pellet the PR inclusion bodies. The inclusion bodies were washed extensively with double-distilled  $\text{H}_2\text{O}$ . The PR inclusion bodies were again pelleted and then solubilized in buffer A (8 M urea, 10 mM Tris [pH 8.0], 5 mM EDTA).

**Protease purification and renaturation.** PR in buffer A was loaded onto a Q Sepharose Fast Flow column (Pharmacia) equilibrated in buffer A. The protein fraction that did not bind to the column was collected, brought to 20 mM sodium acetate (pH 5.0), and adjusted to pH 5.0 with 0.1 M acetic acid. The protein was then loaded onto a Resource S column (Pharmacia) equilibrated in buffer B (8 M urea, 20 mM sodium acetate [pH 5.0], 5 mM EDTA). The PR that bound to the column was eluted with a 0 to 1 M NaCl gradient in 8 M urea. Eluted PR fractions were made 50 mM 3-[cyclohexylamino]-1-propanesulfonic acid (CAPS) (pH 10.5)–0.1 M dithiothreitol (DTT)–150 mM NaCl and dialyzed against buffer D (25 mM  $\text{NaPO}_4$  [pH 7.4], 150 mM NaCl, 5 mM EDTA, 2 mM DTT), using a 6K- to 8K-molecular-weight-cutoff membrane (Spectropore) at  $5^{\circ}\text{C}$  until the urea concentration was  $<5$  mM as described previously (34). The renatured PR solution was then made 5% isopropanol and concentrated to ~1 mg/ml, using an Amicon stirred cell concentrator with a YM 10-kDa-cutoff membrane. The concentrated PR samples were next dialyzed against buffer D to reduce the concentration of isopropanol to  $<0.002\%$  and either stored at  $-70^{\circ}\text{C}$  or brought to 50% glycerol and stored at  $-20^{\circ}\text{C}$ .

**Mass spectrometry.** Protein samples prepared for matrix-assisted laser desorption-ionization/mass spectrometry (MALDI/MS) were mixed with 100% acetonitrile and 0.1% trifluoroacetic acid (TFA) and then diluted 1:2 with a 50% water-acetonitrile solution saturated with 3,5-dimethoxy-4-hydroxy-cinnamic acid (matrix). A 1- $\mu\text{l}$  aliquot of this solution was then dried on the sample holder for analysis with a MALDI mass spectrometer (Ciphergen Biosystem, Inc.). The time-of-flight spectra were internally calibrated with the singly and doubly charged species of the full-length PR detected in each sample.

Soluble PRs analyzed by atmospheric pressure ionization mass spectrometry (API/MS; Perkin-Elmer/Sciex) were first dialyzed against  $\text{H}_2\text{O}$  and then made 30% acetonitrile and 0.1% TFA. The double-distilled  $\text{H}_2\text{O}$ -washed PR inclusion bodies were directly solubilized in 60% acetonitrile–0.1% TFA and then centrifuged at  $10,000 \times g$  for 2 min. The mass of FIV PR and each mutant PR was analyzed by API/MS and was within  $\pm 1$  Da of the calculated molecular mass (data not shown).

**Protease assays.** (i)  **$K_m/k_{\text{cat}}$  determination.** The activities of the various purified PRs were assayed by using a fluorogenic peptide substrate as described previously (7). Briefly, the [PR] was 150 nM in assay buffer (50 mM sodium citrate–100 mM sodium phosphate [pH 5.25], 0.2 M NaCl, 1 mM DTT) containing substrate at concentrations above and below the  $K_m$ . Assays were done in triplicate at  $37^{\circ}\text{C}$ , and data were collected by using a JASCO FP 777 spectrofluorometer.  $K_m$  and  $k_{\text{cat}}$  values were determined by using double-reciprocal Lineweaver-Burk plots (Table 1).

(ii) **Autolysis time course.** The [PR] was either 150 nM or 15  $\mu\text{M}$  in 25 mM  $\text{NaPO}_4$  (pH 7.0)–0.2 M NaCl–1 mM DTT, and PR was incubated at  $37^{\circ}\text{C}$  for 1 to 48 h. Aliquots of the PR autolysis reaction mixture were either made 50% (vol/vol) glycerol at the indicated time points (Fig. 4) and stored at  $-20^{\circ}\text{C}$  or centrifuged with the coprecipitated autolysis products and PR solubilized in 50% acetonitrile for use in MALDI analysis. The 50% glycerol stock of the PR autolysis reaction mixtures were assayed for activity in 100  $\mu\text{l}$  of assay buffer (50 mM NaCl) with fluorogenic substrate (150  $\mu\text{M}$ ) at  $37^{\circ}\text{C}$  for 2 min. Under these saturating substrate conditions, the initial rate of cleavage was determined and used to estimate the amount of PR activity in the reaction. The time zero initial cleavage rate was set to 100% activity for all PRs. Assays were done in triplicate and repeated.

(iii) **Urea inhibition assay.** The PR activity was determined as in the autolysis time course assay except that the assay buffer contained increasing amounts of urea (0.1 to 1.6 M). The initial cleavage rate, in the absence of urea, was set to 100% activity for all PRs. Assays were done in triplicate and repeated.

**Virus propagation.** FIV-34TF10 (30) was propagated in Crandell feline kidney cells. Supernatants from chronically infected cells were harvested at confluency, concentrated, and purified as described previously (6).

**Western blots.** Purified FIV virions and FIV PR in vitro-generated autolysis products were subjected to sodium dodecyl sulfate (SDS)-polyacrylamide gel electrophoresis (PAGE) and transferred to Immobilon-P membranes (Millipore). Each lane was incubated separately with polyclonal anti-PR antibody generated in rabbits against chemically synthesized FIV PR (26). The blots were washed and then again incubated separately with horseradish peroxidase-conjugated anti-rabbit immunoglobulin G (Cappel) and developed by using SuperSignal ULTRA chemiluminescent substrate (Pierce). Molecular weight standards were Mark12 (Novex).

## RESULTS

**Protease expression.** FIV protease is expressed in vivo as part of the Gag/Pol polyprotein and, after autoprocessing out of the polyprotein, has a unit length of 116 amino acids (N-terminal tyrosine, C-terminal methionine [6]). We cloned and expressed the unit-length FIV protease with the addition of a methionine and alanine at the N terminus. This resulted in FIV PR with only an additional alanine on the N terminus with respect to the wild-type PR (Fig. 1, lane 1; Fig. 2). The N-terminal methionine was removed during expression presumably by an *E. coli* methionine amino peptidase (2). In the case of Thr6/PR (see below), the N-terminal methionine was removed, leaving the native threonine (Fig. 2). During the concentration of the renatured FIV PR at  $5^{\circ}\text{C}$ , it was noted that the yield of full-length enzyme decreased as a function of both time and protein concentration. The autolysis products of FIV PR accumulated as a precipitate during renaturation-concentration and were removed by centrifugation. This resulted in the PR being of  $>95\%$  purity as judged by analysis of SDS-polyacrylamide gels stained with Coomassie blue (Fig. 1, lane 1).

**Protease autolysis sites in vitro.** With HIV type 1 (HIV-1), HIV-2, and SIV, the respective proteases have been demon-

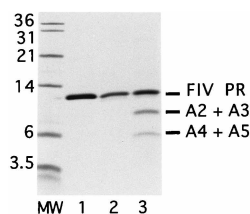


FIG. 1. Coomassie blue-stained SDS-polyacrylamide gel of FIV PR and autolysis products. Lane 1, FIV PR at time zero; lane 2, soluble FIV PR after 20 h at 37°C; lane 3, precipitated autolysis products and coprecipitated FIV PR after 20 h at 37°C. Positions of full-length FIV PR and autolysis products are indicated on the right. MW, molecular weight markers (positions are indicated in kilodaltons on the left).

strated to undergo autolysis (17, 25). Our observations during purification of the FIV PR suggested that it was also undergoing autolysis. To characterize FIV PR autolysis, the purified PR (Fig. 1, lane 1) was incubated at concentrations from 150 nM to 15  $\mu$ M (see Materials and Methods), and the reaction was analyzed by SDS-PAGE (Fig. 1, lane 3) and MALDI/MS (Fig. 3A and B). N-terminal amino acid sequencing was also used to analyze the autolysis products which accumulated during the assay (Fig. 2). Four primary autolysis sites were mapped to FIV PR (Fig. 2) and are indicated in the three-dimensional structure of the PR (Fig. 4A). Cleavage in the Flap (N55/M56), and in the C terminus (Q83/C84 and N88/V89), is predicted to disrupt the FIV PR dimer quaternary structure and consequently PR activity. However, it is not obvious how cleavage at the N-terminal G5/T6 site would affect the PR activity, since it is not part of the core FIV PR dimer (Fig. 4A).

**Protease breakdown products in vivo.** To determine if PR autolysis occurs in virions, purified FIV virions were analyzed by Western blotting for FIV PR breakdown products with a PR-specific antibody (Fig. 5, lane 2). The PR breakdown products found in virions were of the same apparent molecular weight as the in vitro-generated autolysis products (Fig. 5).

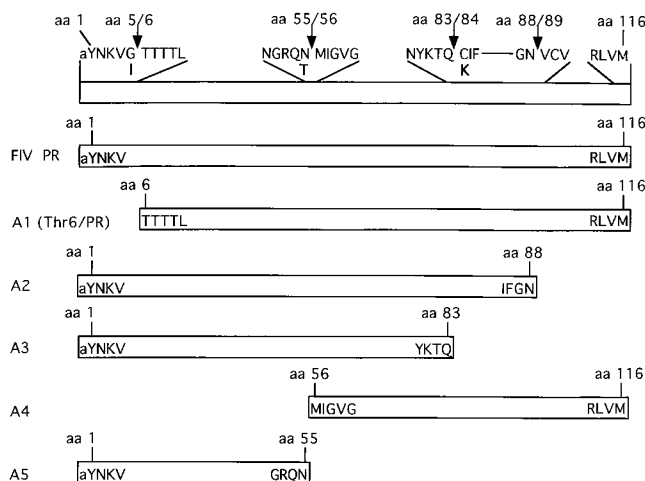


FIG. 2. The FIV PR sequence in single-letter amino acid code is shown at the top. a, nonnative amino acid. Amino acids bordering autolysis sites are indicated; letters below the sequence indicate amino acid substitutions used to block the respective autolysis sites (see Materials and Methods). A1 to A5 autolysis product N-terminal and C-terminal amino acids are indicated. N-terminal amino acids were determined by N-terminal amino acid sequencing and used in conjunction with masses of autolysis products (see the legend to Fig. 3) to determine C-terminal amino acids. A1 is also labeled Thr6/PR.

**Autolysis-resistant proteases.** To block the N-terminal and Flap autolysis sites in the FIV PR, we used a strategy similar to that used for HIV-1 PR (17, 25) in which the cleavage site P1 amino acids were substituted with  $\beta$ -branched amino acids that are not permitted in the HIV-1 PR S1 substrate binding pocket due to steric hindrance (Fig. 2, top) (5). However, for the FIV PR C-terminal Q83/C84 autolysis site, it was noted that HIV-1 PR Lys 70 is found at the same three-dimensional position as the FIV PR C-terminal cleavage site P1' Cys 84 (9, 27). As a result, the C-terminal Q83/C84 cleavage site P1' Cys was substituted with Lys, which is not found in retroviral aspartic protease S2-S2' substrate binding pockets (Fig. 2, top) (21).

To determine the effect of blocking autolysis sites on PR activity, four mutant PRs were constructed and tested (Fig. 2, top): the Flap N55/M56 cleavage site P1 asparagine was substituted with threonine (N55T/PR); the N-terminal G5I and Flap cleavage site mutations were combined (2X/PR); and the N-terminal, Flap, and C-terminal C84K cleavage site mutations were combined (3X/PR). In addition, the PR ORF was truncated by five codons to express the N-terminally truncated form of the PR (Thr6/PR) (Fig. 2).

The FIV PR and mutant PRs were incubated (37°C, pH 7.0, 0.2 M NaCl) and tested over 16 h (Fig. 6) for activity with the fluorogenic substrate in order to quantitate remaining PR activity (Materials and Methods). FIV PR lost  $\sim$ 65% activity in 16 h, with accumulation of the corresponding C-terminal (A2 and A3) and Flap (A4 and A5) cleavage products as determined by SDS-PAGE (Fig. 1, lane 3) and MALDI/MS (Fig. 3A). In the case of N55T/PR, in which the Flap cleavage site was blocked, there was a loss of only  $\sim$ 25% activity in 16 h (Fig. 6). However, the MALDI/MS data indicated that N55T/PR cleaved at the N-terminal cleavage site, resulting in the N-terminally truncated form of the PR (Thr6/PR, autolysis product A1 [Fig. 2]), as well as at the C-terminal Q83/C84 and N88/V89 cleavage sites, giving the respective A3 and A2 autolysis products (Fig. 2 and 3). In the case of the double mutant 2X/PR, both the mutated N-terminal and Flap autolysis sites were protected, resulting in a PR which lost  $\sim$ 25% activity over the 16-h time course (Fig. 6). The C-terminal cleavage sites in 2X/PR were not protected (Fig. 3A). The mutant 3X/PR, which contained the three blocked autolysis sites, was highly resistant to autolysis, with no significant loss in activity after 16 h (Fig. 3A and 6). Interestingly, the C84K mutation, which blocked the Q83/C84 site, also blocked the N88/V89 site in 3X/PR (Fig. 3A). The D30N/PR active-site mutant served as a negative control in that it can bind substrate (15a) but is inactive and so cannot generate autolysis products (Table 1; Fig. 3C).

**Protease enzymatic activity.** The kinetic parameters  $K_m$  and  $k_{cat}$  were determined for the FIV PR and mutant PRs. The values obtained for the autolysis-resistant mutants were similar to those for FIV PR, with one exception: Thr6/PR had an increase in  $k_{cat}$  (Table 1) and was resistant to autolysis (Fig. 6). To test if the Thr6/PR increase in  $k_{cat}$  was due to an increase in the PR dimer/monomer ratio, FIV PR, Thr6/PR, and 3X/PR were assayed for activity in increasing concentrations of urea. Thr6/PR retained four times more activity than FIV PR and 3X/PR when 1.2 M urea was included in the assay buffer (Fig. 7).

## DISCUSSION

The FIV protease is activated during budding of immature virions, resulting in the maturation of infectious virus, and may play other roles in post-virion maturation events (1, 24). In this study, we have demonstrated that the FIV PR undergoes au-

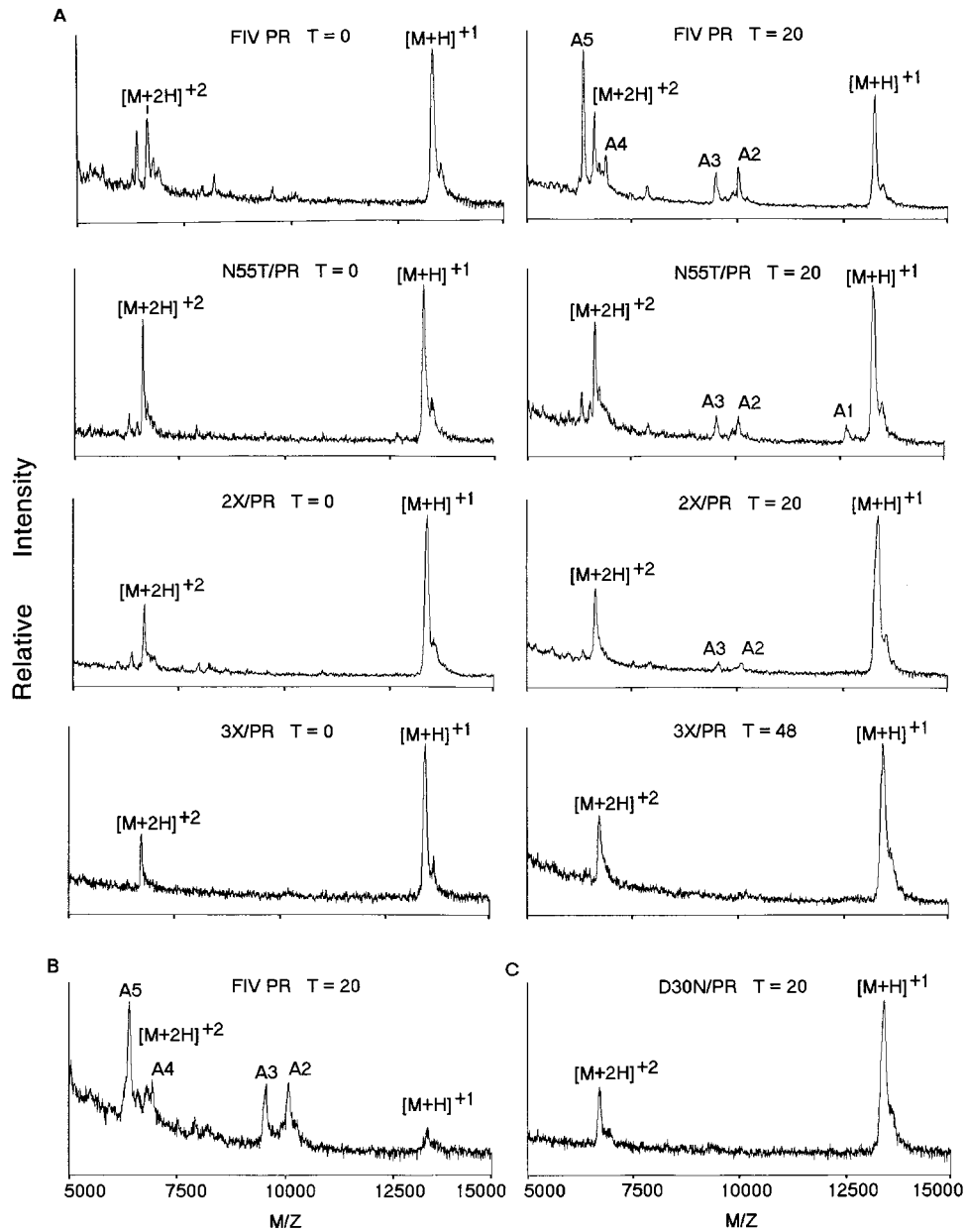


FIG. 3. MALDI/MS analysis of FIV PR and autolysis-resistant forms of the PR at time zero and after either 20 h ( $T = 20$ ) or 48 h ( $T = 48$ ). The autolysis products form a precipitate and do not quantitatively resuspend; as a result, the data are only qualitative. The singly  $[M+H]^{1+}$  and doubly  $[M+2H]^{2+}$  charged forms of the full-length PRs are indicated and were used to calibrate the respective spectrums. The determined/calculated masses (in daltons) of the autolysis products A1 to A5 are given in brackets below for the PRs. (A) All PRs were at  $15 \mu\text{M}$  in the autolysis assay. Shown are results for FIV PR (A2 [10,075/10,078], A3 [9,546/9,543], A4 [6,923/6,923], and A5 [6,393/6,398]), N55T/PR (A1 [12,657/12,659], A2 [10,068/10,065], and A3 [9,540/9,530]), and 2X/PR (A2 [10,114/10,121] and A3 [9,587/9,586]). There were no autolysis products, or precipitate, with 3X/PR. (B) FIV PR as in panel A except that FIV PR was at  $150 \text{ nM}$  in the autolysis assay (A2 [10,075/10,073], A3 [9,546/9,548], A4 [6,923/6,939], and A5 [6,393/6,407]). (C) D30N/PR. The active-site aspartic acid was mutated to asparagine, inactivating protease.

tolysis in vitro. To confirm that the autolysis that we observed with the PR was not due to expression in *E. coli* or of high in vitro concentrations of enzyme, we performed three experiments to address these issues. First, we showed that an inactive mutant PR (D30N/PR) expressed and purified under identical conditions did not undergo autolysis (Fig. 3C). Thus, FIV PR autolysis is not due to a contaminating *E. coli* protease. Second, we analyzed purified FIV virions by Western blot analysis to determine if similar autolysis products could be identified during normal virus expression. The results, shown in Fig. 5, demonstrated that PR breakdown products of the same appar-

ent molecular weights as autolysis products generated in vitro were present in virions. Third, we performed autolysis reactions with PR at concentrations ranging from  $15 \mu\text{M}$  to  $150 \text{ nM}$ . The results show that the same autolysis products were generated regardless of concentration (Fig. 3A and B), supporting the conclusion that PR autolysis involves specific recognition of high-affinity cleavage sites.

Autolysis occurs at four primary sites in FIV PR: (i) near the N terminus (G5/T6), (ii) in the Flap (N55/M56), (iii) in the C terminus (Q83/C84), and (iv) in the C terminus (N88/V89) (Fig. 2 and 4A). Cleavage in the Flap and C terminus results in

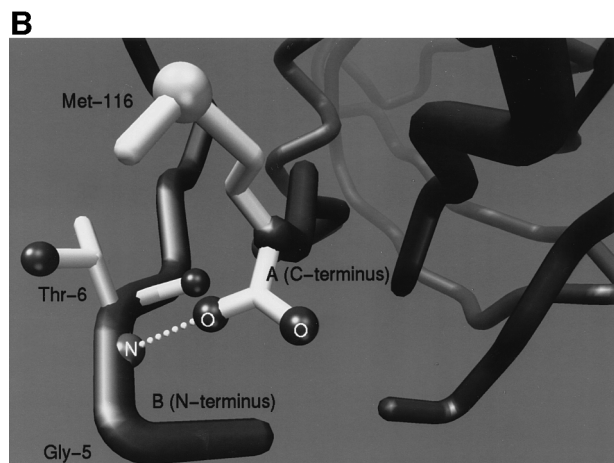
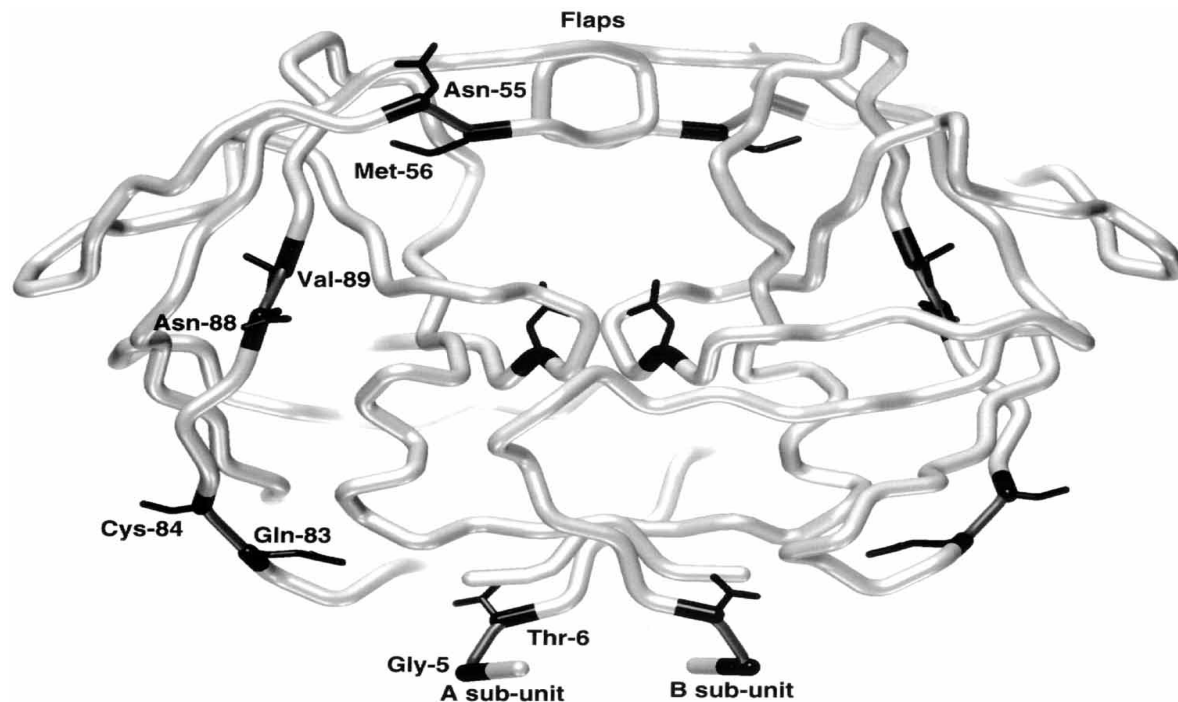


FIG. 4. (A) Three-dimensional structure of the FIV PR, with the four autolysis sites in black. For clarity, only the amino acid side chains bordering the scissile bonds are indicated. The N-terminal three amino acids are disordered in the crystal structure and so not shown. The active-site aspartic acids (center) are in black. (B) View of the N and C termini of the dimer from the right side of panel A. The backbone nitrogen (N) of Thr 6 from the B subunit and C-terminal oxygen (O) from the A subunit are predicted to form the hydrogen bond shown with white dots. A-subunit C-terminal Met 116 is indicated.

inactivation of the PR (autolysis products precipitate [Fig. 1, lane 3]) and may be important in degradation of the PR in vivo, while cleavage near the N terminus (which removes five native amino acids from the FIV PR) results in a truncated Thr6/PR (Fig. 2 and 3A) which is resistant to autolysis (Fig. 6) and retains four times more activity than FIV PR in 1.2 M urea (Fig. 7). These findings are consistent with Thr6/PR having increased dimer stability and likely explain the increase observed in  $k_{cat}$  (Table 1).

Analysis of the autolysis-resistant PRs determined that autolysis sites were blocked with the respective P1 or P1' amino acid substitutions. The N55/M56 Flap cleavage site was blocked in N55T/PR, though autolysis was predictably not blocked at the unmodified N-terminal and C-terminal cleavage sites (Fig. 3A). In addition, Thr6/PR (autolysis product A1 [Fig. 2]) accumulated in the N55T/PR autolysis reaction, suggesting that blocking the Flap cleavage site made the N-terminal cleavage site more favorable (Fig. 3A). The accumulation of Thr6/PR with a higher  $k_{cat}$  in the N55T/PR autolysis reac-

tion may explain why even though the N55T/PR is breaking down (Fig. 3A), the reaction retains significantly more activity over the 16-h autolysis time course than FIV PR (Fig. 6). Blocking all four primary autolysis sites in 3X/PR results in an enzyme which is similar in kinetics and stability in urea to FIV PR (Table 1; Fig. 7) but is highly resistant to autolysis (Fig. 3A and 6). Since evolution could have yielded a PR resistant to autolysis, with retention of wild-type activity, these results imply that the autolysis sites may have been positively selected for in the PR for activity regulation.

Since purified FIV virions contain PR breakdown products similar in mass to the in vitro-generated autolysis products (Fig. 5), we conclude that PR autolysis may play a role in regulation of PR activity in vivo. However, since the N-terminal G5/T6 autolysis site is cleaved slowly to generate Thr6/PR, it may represent a remnant cleavage site that had been used to cleave the N terminus of the PR out of the Gag/Pol polypro-

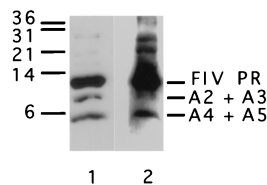


FIG. 5. Western blot analysis of FIV PR and in vitro-generated autolysis products (lane 1) and of purified FIV virions (lane 2) with an FIV PR-specific antibody. Positions of FIV PR and autolysis products are indicated on the right. Positions of molecular weight markers are indicated in kilodaltons on the left.

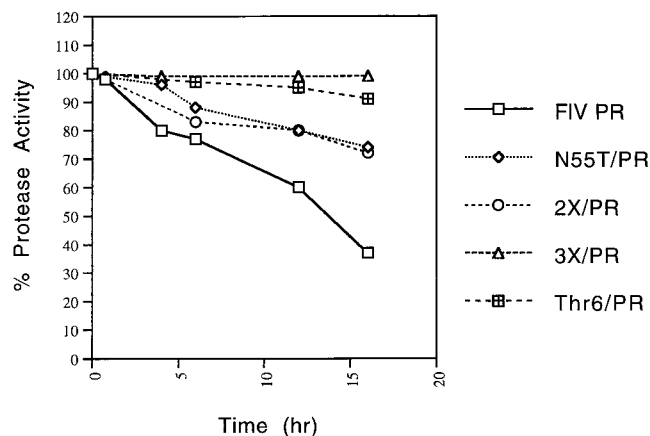


FIG. 6. FIV PR and mutant PR activities at indicated time points during the autolysis assay.

tein. After the site was mutated and blocked, the new N-terminal cleavage site resulted in an extended N terminus which destabilized the PR dimer, allowing the resulting monomers to undergo autolysis and so increase the rate of PR inactivation. It is notable that the backbone nitrogen between G5/T6 in the FIV PR B subunit can make a hydrogen bond with the C-terminal oxygen in the FIV PR A subunit, and vice versa (Fig. 4B). Subsequent cleavage at the G5/T6 junctions results in the threonine 6 backbone nitrogen becoming an N-terminal nitrogen ( $H_3N^+$ ) which can make a salt bridge with the corresponding C-terminal oxygen ( $COO^-$ ). These stronger bonds may be responsible for stabilizing the Thr6/PR dimer against autolysis and urea inhibition and for increasing the  $k_{cat}$  via an increase in the dimer/monomer ratio. In an earlier construct in which Thr6/PR had an additional Ala on the N terminus, the PR had a stability similar to that of FIV PR (data not shown). HIV-1 PR, when processed out of the Gag/Pol polyprotein, is predicted to form salt bridges similar to those of Thr6/PR between the N termini and C termini of the respective subunits (32).

In the case of pepsin, a mammalian gastric protease, the inactive zymogen (pepsinogen) is secreted from the cells lining the stomach. An acidic environment in the gut then activates

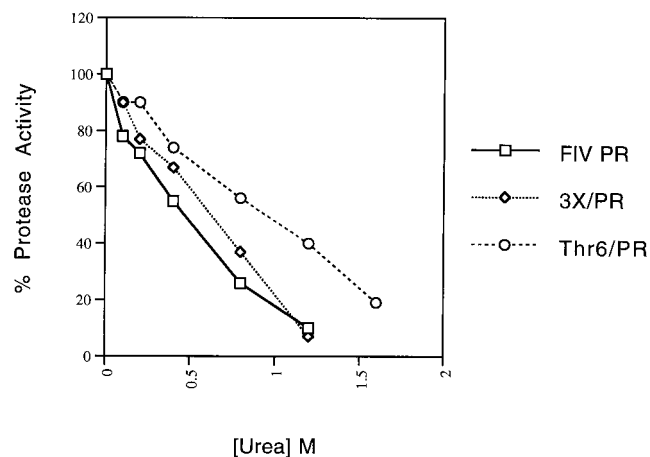


FIG. 7. Effect of urea concentration on FIV PR and mutant PR initial rates of cleavage.

TABLE 1. FIV PR and mutant PR activities

Protease	Mean $\pm$ SD		
	$k_{cat}$	$K_m$	$k_{cat}/K_m$
FIV PR	$0.38 \pm 0.02$	$33 \pm 5$	$0.0115 \pm 0.0010$
N55T/PR	$0.36 \pm 0.05$	$49 \pm 10$	$0.0073 \pm 0.0005$
2X/PR	$0.34 \pm 0.04$	$45 \pm 6$	$0.0075 \pm 0.0005$
3X/PR	$0.32 \pm 0.05$	$53 \pm 12$	$0.0060 \pm 0.0005$
Thr6/PR	$0.60 \pm 0.05$	$37 \pm 4$	$0.0162 \pm 0.0005$
D30N/PR	ND <sup>a</sup>	ND	

<sup>a</sup> ND, not detected.

the zymogen to autoprocess near the N terminus to give the unit-length pepsin (8, 11, 22). While autolysis results in degradation of pepsin in vitro (8, 22), it may also be important in removing the inherently nonspecific protease from the gut and so minimizing degradation of the cells lining the stomach (16, 31). Similar to pepsinogen, viral aspartyl proteases are also activated due to a change in the local environment, resulting in the autoprocessing of the PRs out of a polyprotein (4, 23). Subsequently, the unit-length HIV-1, HIV-2, and SIV PRs have been shown to undergo autolysis, initially near the N terminus, resulting in inactivation of the PRs in vitro (17, 25). In the case of FIV PR, cleavage near the extended N terminus increases the activity and stability of the PR (Table 1; Fig. 6). The remaining autolysis sites in FIV PR are located in  $\beta$  sheet/hairpins/ $\beta$  sheets ( $\beta$  hairpins), perhaps making them accessible in the monomer. Several autolysis sites in the HIV-1, HIV-2, and SIV PRs are also in  $\beta$  hairpins (25).

With FIV, roles of the PR after virion maturation have not been described. However, HIV-1 PR has been shown to degrade inhibitor-resistant forms of HIV-1 reverse transcriptase in mature virions, resulting in decreased viral infectivity (18). HIV-1 PR can also partially degrade the Nef protein in virions (33). While equine infectious anemia virus PR can degrade the nucleocapsid protein in virions in vitro, this could affect initiation of reverse transcription in vivo (19). Together, these results indicate that retroviral PRs can partially degrade key viral proteins in the virion and suggest that inactivation of the PR in vivo through autolysis may limit further degradation of the mature viral proteins. The fact that FIV virions contain PR breakdown products lends support to autolysis playing a role in PR inactivation in vivo.

During virion entry and initiation of the replication cycle in a newly infected cell, the continued presence of 100 to 200 PRs/virion within the cell may ultimately have an adverse effect on virus replication. The ability of retroviral PRs to undergo autolysis could be important in removing the PR activity so that de novo-synthesized Gag and Gag/Pol polyproteins are not prematurely processed by the exogenous PR from infecting virus but are targeted to the plasma membrane for virion assembly (12, 14, 15). The role of autolysis in inactivation of FIV PR can now be tested ex vivo by expressing autolysis-resistant PRs, using recombinant FIVs in cell cultures.

#### ACKNOWLEDGMENTS

We thank Danica L. Lerner for purified FIV. We also thank Alexander Wlodawer and Alla Gustchina for thoughtful discussions; Tilman M. Hackeng, John M. Louis, and Sergei Gulnik for advice and insight; and Aymeric de Parserval for careful review of the manuscript.

This research was supported by funds from the National Institutes of Health (RO1 AI40882-01 and 5 PO1 GM48870). G.S.L. was supported by a National Institutes of Health training grant. M.C.F. was the recipient of a National Research Service Award sponsored by the National Institutes of Health.

## REFERENCES

1. Baboonian, C., A. Dagleish, L. Bountiff, J. Gross, S. Oroszlan, G. Rickett, C. Smith-Burchnell, P. Troke, and J. Merson. 1991. HIV-1 protease is required for synthesis of pro-viral DNA. *Biochem. Biophys. Res. Commun.* **179**:17–24.
2. Ben-Bassat, A., K. Bauer, S. Y. Chang, K. Myambo, A. Boosman, and S. Chang. 1987. Processing of the initiation methionine from proteins: properties of the *Escherichia coli* methionine aminopeptidase and its gene structure. *J. Bacteriol.* **169**:751–757.
3. Bryant, M. L., L. Ratner, R. J. Duronio, N. S. Kishore, B. Devadas, S. P. Adams, and J. I. Gordon. 1991. Incorporation of 12-methoxydodecanoate into the human immunodeficiency virus 1 gag polyprotein precursor inhibits its proteolytic processing and virus production in a chronically infected human lymphoid cell line. *Proc. Natl. Acad. Sci. USA* **88**:2055–2059.
4. Coffin, J. M. 1996. Retroviridae: the viruses and their replication, p. 1767–1847. In B. N. Fields, D. M. Knipe, P. M. Howley, et al. (ed.), *Fields virology*, 3rd ed. Lippincott-Raven, Philadelphia, Pa.
5. Dunn, B., A. Gustchina, A. Wlodawer, and J. Kay. 1994. Substrate specificity and inhibitor design, p. 254–278. In L. C. Kuo and J. A. Schafer (ed.), *Retroviral proteases*. Academic Press, Inc., San Diego, Calif.
6. Elder, J. H., M. Schnolzer, C. S. Hasselkus-Light, M. Henson, D. A. Lerner, T. R. Phillips, P. C. Wagaman, and S. B. H. Kent. 1993. Identification of proteolytic processing sites within the Gag and Pol polyproteins of feline immunodeficiency virus. *J. Virol.* **67**:1869–1876.
7. Fitzgerald, M. C., G. S. Laco, J. H. Elder, and S. B. H. Kent. Submitted for publication.
8. Fruton, J. S. 1971. Pepsin, p. 120–152. In P. D. Boyer (ed.), *Hydrolysis: peptide bonds*. Academic Press, New York, N.Y.
9. Gustchina, A., J. Kervinen, D. J. Powell, A. Zdanov, J. Kay, and A. Wlodawer. 1996. Structure of equine infectious anemia virus proteinase complexed with an inhibitor. *Protein Sci.* **5**:1453–1465.
10. Henderson, L. E., M. A. Bowers, R. C. I. Sowder, T. D. Copeland, G. Smythers, and S. Oroszlan. 1992. Gag proteins of the highly replicative MN strain of human immunodeficiency virus type 1: posttranslational modifications, proteolytic processings, and complete amino acid sequences. *J. Virol.* **66**:1856–1865.
11. James, M. N. G., and A. R. Sielecki. 1986. Molecular structure of an aspartic proteinase zymogen, porcine pepsinogen, at 1.8 Å resolution. *Nature* **319**:33–38.
12. Karacostas, V., E. J. Wolffe, K. Nagashima, M. A. Gonda, and B. Moss. 1993. Overexpression of the HIV-1 Gag-Pol polyproteins result in intracellular activation of HIV-1 protease and inhibition of assembly and budding of virus-like particles. *Virology* **193**:661–671.
13. Kohl, N. E., E. A. Emilio, W. A. Schleif, L. J. Davis, J. C. Heimbach, R. A. F. Dixon, E. M. Scolnick, and I. S. Sigal. 1988. Active human immunodeficiency virus protease is required for viral infection. *Proc. Natl. Acad. Sci. USA* **85**:4686–4690.
14. Kräusslich, H. G. 1991. Human immunodeficiency virus proteinase dimer as component of the viral polyprotein prevents particle assembly and viral infectivity. *Proc. Natl. Acad. Sci. USA* **88**:3213–3217.
15. Kräusslich, H. G. 1992. Specific inhibitor of human immunodeficiency virus proteinase prevents the cytotoxic effects of a single-chain proteinase dimer and restores particle formation. *J. Virol.* **66**:567–572.
- 15a. Laco, G. S., C. Schalk-Hihi, J. Lubkowski, G. M. Morris, A. Zdanov, A. J. Olson, J. H. Elder, A. Wlodawer and A. Gustchina. Submitted for publication.
16. Matuz, J. 1992. Role of mucus in mucosal protection through ethanol and pepsin damage models. *Acta Physiol. Hung.* **80**:189–194.
17. Mildner, A. M., D. J. Rothrock, J. W. Leone, C. A. Bannow, J. M. Lull, I. M. Reardon, J. L. Sarcich, W. J. Howe, C. S. C. Tomich, C. W. Smith, R. L. Heinrikson, and A. G. Tomasselli. 1994. The HIV-1 protease as enzyme and substrate: mutagenesis of autolysis sites and generation of a stable mutant with retained kinetic properties. *Biochemistry* **33**:9405–9413.
18. Olmsted, R. A., D. E. Slade, L. A. Kopta, S. M. Poppe, T. J. Poel, S. W. Newport, K. B. Rank, C. Biles, R. A. Morge, T. J. Dueweke, Y. Yagi, D. Romero, R. C. Thomas, S. K. Sharma, and W. G. Tarpley. 1996. (Alkylamino)piperidine bis(heteroaryl)piperazine analogs are potent, broad-spectrum nonnucleoside reverse transcriptase inhibitors of drug-resistant isolates of human immunodeficiency virus type 1 (HIV-1) and select for drug-resistant variants of HIV-1<sub>IIIB</sub> with reduced replication phenotypes. *J. Virol.* **70**:3698–3705.
19. Oroszlan, S. 1989. Biosynthesis and proteolytic processing of retroviral proteins: an overview, p. 87–100. In S. Oroszlan and E. Wimmer (ed.), *Viral proteinases as targets for chemotherapy*. Cold Spring Harbor Laboratory Press, Cold Spring Harbor, N.Y.
20. Pedersen, N. C., E. W. Ho, M. L. Brown, and J. K. Yamamoto. 1987. Isolation of a T-lymphotropic virus from domestic cats with an immunodeficiency-like syndrome. *Science* **235**:790–793.
21. Poorman, R. A., A. G. Tomasselli, R. L. Heinrikson, and F. J. Kezdy. 1991. A cumulative specificity model for proteases from human immunodeficiency virus types 1 and 2, inferred from statistical analysis of an extended substrate data base. *J. Biol. Chem.* **266**:14554–14561.
22. Rajagopalan, T. G., S. Moore, and W. H. Stein. 1966. Pepsin from pepsinogen. *J. Biol. Chem.* **241**:4940–4950.
23. Ratner, L. 1993. HIV life cycle and genetic approaches. *Perspect. Drug Discov. Des.* **1**:3–22.
24. Roberts, M. M., T. D. Copeland, and S. Oroszlan. 1991. *In situ* processing of a retroviral nucleocapsid protein by the viral proteinase. *Protein Eng.* **4**:695–700.
25. Rose, J. R., R. Salto, and C. S. Craik. 1993. Regulation of autoproteolysis of the HIV-1 and HIV-2 proteases with engineered amino acid substitutions. *J. Biol. Chem.* **268**:11939–11945.
26. Schnolzer, M., H. R. Rackwitz, A. Gustchina, G. S. Laco, A. Wlodawer, J. H. Elder, and S. B. H. Kent. 1996. Comparative properties of feline immunodeficiency virus (FIV) and human immunodeficiency virus type 1 (HIV-1) proteinases prepared by total chemical synthesis. *Virology* **224**:268–275.
27. Slee, D. H., K. L. Laslo, J. H. Elder, I. R. Oilmann, A. Gustchina, J. Kervinen, A. Zdanov, A. Wlodawer, and C. H. Wong. 1995. Selectivity in the inhibition of HIV and FIV protease: inhibitory and mechanistic studies of pyrrolidine-containing  $\alpha$ -keto amide and hydroxyethylamine core structures. *J. Am. Chem. Soc.* **117**:11867–11878.
28. Studier, F. W., A. H. Rosenberg, J. J. Dunn, and J. W. Dubendorff. 1990. Use of T7 RNA polymerase to direct expression of cloned genes. *Methods Enzymol.* **185**:60–89.
29. Tabor, S., and C. C. Richardson. 1985. A bacteriophage T7 RNA polymerase/promoter system for controlled exclusive expression of specific genes. *Proc. Natl. Acad. Sci. USA* **82**:1074–1078.
30. Talbot, R. L., E. E. Sparger, K. M. Lovelace, W. M. Fitch, N. C. Pederson, P. A. Luciw, and J. H. Elder. 1989. Nucleotide sequence and genome organization of feline immunodeficiency virus. *Proc. Natl. Acad. Sci. USA* **86**:5743–5747.
31. Vaezi, M. F., S. Singh, and J. E. Richter. 1995. Role of acid and duodenogastric reflux in esophageal mucosal injury: a review of animal and human studies. *Gastroenterology* **108**:1897–1907.
32. Weber, I. T. 1990. Comparison of the crystal structures and intersubunit interactions of human immunodeficiency and Rous sarcoma virus proteases. *J. Biol. Chem.* **265**:10492–10496.
33. Welker, R., H. Kottler, H. R. Kalbitzer, and H. G. Krausslich. 1996. Human immunodeficiency virus type 1 nef protein is incorporated into virus particles and specifically cleaved by the viral proteinase. *Virology* **219**:228–236.
34. Wlodawer, A., A. Gustchina, L. Reshetnikova, J. Lubkowski, A. Zdanov, K. Y. Hui, E. L. Angelton, W. G. Farmerie, M. M. Goodenow, D. Bhatt, L. Zhang, and B. M. Dunn. 1995. Structure of an inhibitor complex of the proteinase from feline immunodeficiency virus. *Nat. Struct. Biol.* **2**:480–488.